Investigating plastic deformation around a reheat-crack in a 316H austenitic stainless steel weldment by misorientation mapping

Conference or Workshop Item

Available online at www.sciencedirect.com

ScienceDirect

Procedia Structural Integrity 2 (2016) 3501–3507

Structural Integrity Procedia

www.elsevier.com/locate/procedia

21st European Conference on Fracture, ECF21, 20-24 June 2016, Catania, Italy

Investigating plastic deformation around a reheat-crack in a 316H austenitic stainless steel weldment by misorientation mapping

Rahul Unnikrishnan *, Shirley M. Northover, Hedieh Jazaeri, P. John Bouchard

Materials Engineering, The Open University, Milton Keynes, MK7 6AA, United Kingdom

Abstract

Creep degradation in austenitic stainless steels is associated with nucleation and growth of cavities that can link up to form micro- and macro-cracks, usually along grain boundaries. A reheat crack found near a header nozzle weld removed from a nuclear power station has been examined using both electron backscatter diffraction (EBSD) and hardness mapping. The EBSD studies revealed higher levels of lattice misorientation towards the weld region where the crack initiated with strain particularly concentrated at grain boundaries. The pattern of deformation shown by the EBSD measurements was confirmed by the hardness survey.

Peer-review under responsibility of the Scientific Committee of PCF 2016.

Keywords: Reheat crack; 316H; Austenitic stainless steel; EBSD; Creep cavity

1. Introduction

Intergranular reheat cracks can form in the heat affected zone (HAZ) of non stress relieved type 316H austenitic stainless steel welds during post weld heat treatment or when exposed to operating temperatures in the range of 500 to 700° C. At these temperatures, precipitation of carbides strengthens the grain interiors which prevents plastic deformation within the grains while relaxation of residual stress in the HAZ results in conversion of elastic strain to creep strain. When the material cannot accommodate these effects, cavities form and later link up to form first micro- and then macro- cracks (Bouchard et al., 2004; Skelton et al., 2003).

Published literature on reheat cracking has focused on examining the influence of stress, triaxiality and pre-strain on creep ductility but little attention has been given to the inelastic strain distribution around such cracks. A better understanding of the mechanisms of reheat crack initiation and growth at the microstructural level is required to improve life assessment methods at high temperature for weldments susceptible to reheat cracking. Some insight into the failure mechanisms can be obtained by

* Corresponding author. Tel.: +44-7590075849
E-mail address: rahul.unnikrishnan@open.ac.uk, rahulunnikrishnannair@gmail.com

Peer review under responsibility of the Scientific Committee of PCF 2016.
10.1016/j.prostr.2016.06.436

studying the extent and pattern of plastic deformation in individual grains around a reheat crack as the nominal macroscopic strain, cannot account for local changes in a material's properties such as variable dislocation density and local hardening.

Electron backscatter diffraction (EBSD) is a promising tool in studying the strain distribution in metals at a microstructural level (Fujiyama et al., 2009a, 2009b; Shigeyama et al., 2014; Subedi et al., 2015). In this method, the accumulated inelastic strain is calculated from measurements of surface changes in the local crystallographic orientation ('misorientations'). These lattice rotations are caused by the accumulation of geometrically necessary dislocations (GNDs) which accommodate plastic deformation. Many studies have shown a good correlation between the degree of misorientation and the macroscopic strain in the material but strain measurement using local misorientations is not yet standardised. Various EBSD misorientation metrics can be displayed in the form of maps showing the degree of plastic deformation (Brewer et al., 2006; Jin et al., 2013; M'Saoubi and Ryde, 2005). Maps of micro-hardness have also been successfully used in several studies to show the extent of plastic deformation.

2. Materials and Methods

2.1. Material

The material used for this study was from a steam header nozzle (part of a superheater used to convert saturated or wet steam into dry steam in a power plant). The header was made from AISI Type 316H austenitic stainless steel (HRA 2B2/1 cast 69431). It had been in service for 90,930 hours at a mean temperature of 516°C and under an internal steam pressure of around 16MPa. The component's internal diameter and thickness were 304.8mm and 63.5mm respectively. A diagram of the component can be found elsewhere (Jazaeri et al., 2015). The header had been removed from service in the year 2000 following discovery of a reheat crack near the nozzle weld. The composition of the service-aged material used in the study is:

Table 1. Chemical composition (wt. %) of service-aged Type 316H stainless steel.

C	Si	Mn	P	S	Cr	Ni	Mo	Al	Cu
0.066	0.42	1.00	0.029	0.015	17.82	11.81	2.33	0.003	0.23
Sn	V	W	Co	Pb	B	N	Nb	Ti	Fe
0.016	0.031	0.068	0.093	0.003	0.0051	0.096	0.007	0.004	Bal.

2.2. Microstructure examination

The microstructures were examined with a Leica DMI 5000M reflected light optical microscope using the bright field mode. Higher magnification observations and EBSD measurements were made using a Zeiss Supra 55VP FEGSEM with a NordlysF EBSD detector. The EBSD data were acquired at an accelerating voltage of 20keV, a working distance of 15±0.1mm and a step size of 2μm on a square grid pattern using HKL fast acquisition software. A 70° pre-tilted sample holder was used. EBSD measurements were made at three locations (1) at the crack mouth, near the weld, (2) mid-way along the crack, around 8mm from its mouth and (3) at the crack tip. EBSD measurements of deformation were also made on an area far from the crack for comparison. A minimum of 600,000 data points covering an area of at least 1.4mm^2 was recorded in each EBSD scan.

Samples for both optical microscopy and EBSD were prepared using conventional metallographic procedures of wet grinding on successive grades of silicon carbide papers followed by polishing using successively finer diamond suspensions. The final preparation was electro-polishing at room temperature in Struers A21 electrolyte for 60 s at 22V potential. This produced a specimen surface free of any preparation-induced deformation.

The EBSD parameters Kernel Average Misorientation (KAM) and Grain Reference Orientation Deviation (GROD) were used to evaluate plastic strain at each point. In KAM, the mean misorientation between each measurement point and its neighbours is calculated, excluding any high angle boundaries (HAGBs). (In this case a 3x3 kernel was used, including 8 neighbours for each point and HAGBs were defined by misorientations >15°). KAM maps highlight local strain variations, and KAM values are independent of the grain size. The GROD at any point is the misorientation between that point and the average misorientation of the grain. While KAM considers only misorientations in a small local neighbourhood within a grain, GROD considers local variations in grain scale deformation. In GROD maps the average orientation for the grain is calculated, then each point is shaded according the misorientation it makes relative to the average for the grain (Fujiyama et al., 2015, 2009b; Shigeyama et al., 2014; Subedi et al., 2015).

Micro-hardness measurements were also carried out, following ASTM E384-89 standards, on the surface prepared for EBSD, using a Duramin-A300 hardness tester, at room temperature, with a standard indenter and a load of 2kg. Indentations 0.5mm apart were made around the crack.

3. Results and Discussion

3.1 Microstructural overview

Optical observations revealed the crack to be intergranular (see Fig. 1) and around 16.8mm long. It started from boundaries between grains in the HAZ near the weld. The crack was not continuous but branched and fragmented [see Fig. 1 and 2(c)]. SEM images in the region of the crack near the weld and near the crack tip are shown in Figs 3 and 4 respectively. Cavities around intergranular precipitates along the grain boundaries can be seen, as previously reported for this component (Bouchard et al., 2004; Jazaeri et al., 2014). EBSD orientation maps (IPF colouring) suggest that the grains around the crack are randomly orientated (see Fig. 2).

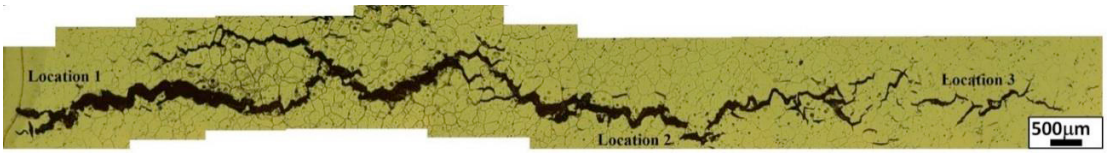

Figure 1. Optical microstructure of the reheat crack.

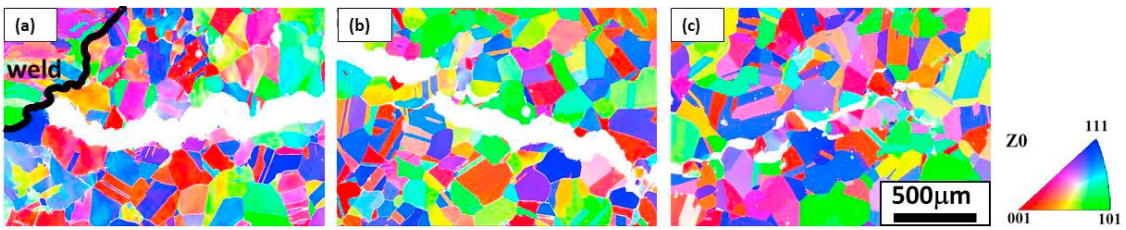

Figure 2. Orientation maps of reheat crack at (a) location 1, (b) location 2 and (c) location 3. Scale bar applies to all images.

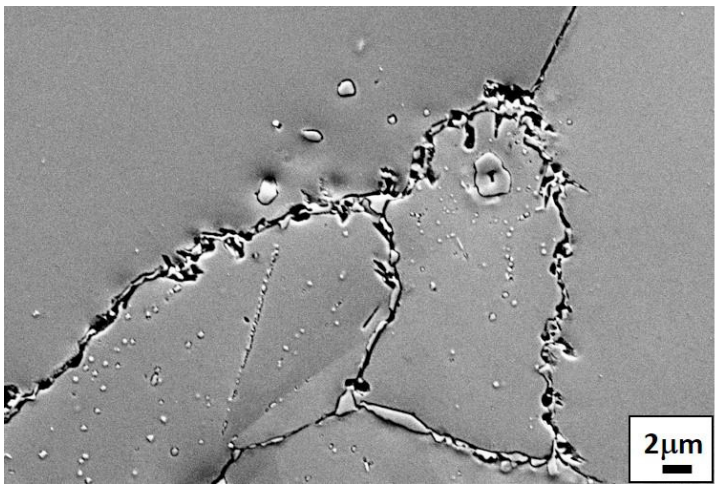

Figure 3. Secondary electron image of grains near the crack tip at location of high KAM and GROD.

3.2 Strain mapping using EBSD

Plastic strain within grains results in local misorientation changes which can be visualised using appropriate EBSD maps (Fujiyama et al., 2009b; Shigeyama et al., 2014; Subedi et al., 2015). These EBSD maps can also be used to analyse the local strain accumulation in the grains semi-quantitatively.

The accommodation of strain by lattice rotations can be visualised in so-called ‘grain boundary’ maps. Fig. 4 shows point to point misorientations >2°, those in the range $2 < \theta < 15°$ being identified by the EBSD software as ‘low angle grain boundaries’

(LAGBs) and those >15° as HAGBs. Regions with high concentrations of LAGBs correspond to areas of high dislocation density (Gottstein and Shvindlerman, 2010). From Fig. 4(a) and (c) it's evident that highly dislocated regions are present in the crack path and especially near the weld in the region where the crack is believed to have initiated.

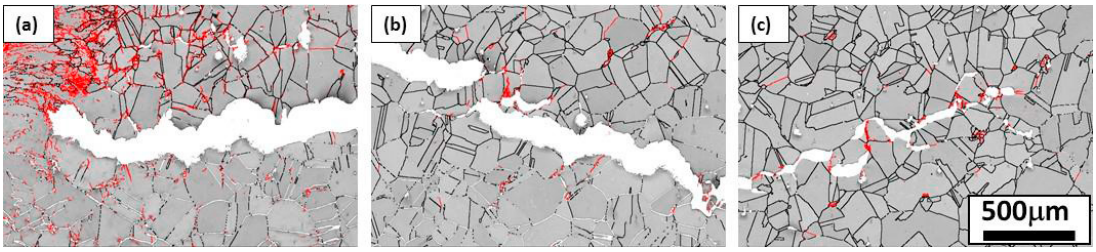

Figure 4. 'Grain boundary' maps of the reheat crack at (a) location 1, (b) location 2 and (c) location 3 (black lines are high angle boundaries [θ > 15º] and red lines are 'low angle boundaries' [2° < θ < 15°]). Micron bar applies to all images.

Fig. 5 shows KAM or local misorientation values at three locations along the reheat crack. In EBSD a grain is defined as a region surrounded by boundaries with a crystal misorientation greater than 15°. KAM usually considers only misorientations less than 2°. KAM values are high at location 1 (the region of crack initiation) implying a high dislocation density in this area. Although KAM values are not absolute, because they depend on the step-size (Githinji et al., 2013), KAM has been shown to be a good measure of GND density (Fujiyama et al., 2009a). The frequency of low KAM values (less than 0.2°) is highest in the areas of the crack remote from the weld whereas high KAM values (up to 1.2°) are evident near the weld (see Fig. 6). The accumulation of dislocations along grain boundaries far from the crack can be detected by both grain boundary and KAM maps (Engler and Randle, 2010). Fujiyama et al. (Fujiyama et al., 2009b) found in high chromium heat resistant steels and weldments that the local KAM values were higher around creep voids due to strain accumulation around them. KAM maps have revealed complex strain localization around voids in many studies (Schwartz et al., 2010). Here, unsurprisingly, both KAM and 'grain boundary' maps show more intense deformation at the grain boundaries near the crack This can be attributed to the inelastic strain accumulation around the voids (Fujiyama et al., 2009b). Both KAM and 'grain boundary' maps showed more intense deformation at the grain boundaries near the crack. Higher resolution (0.1μm step size) KAM maps (for example, see Fig. 7) in the region of micro-cracking show localised regions of large misorientations but cannot be compared quantitatively with the lower magnification maps presented earlier because of the different step size.

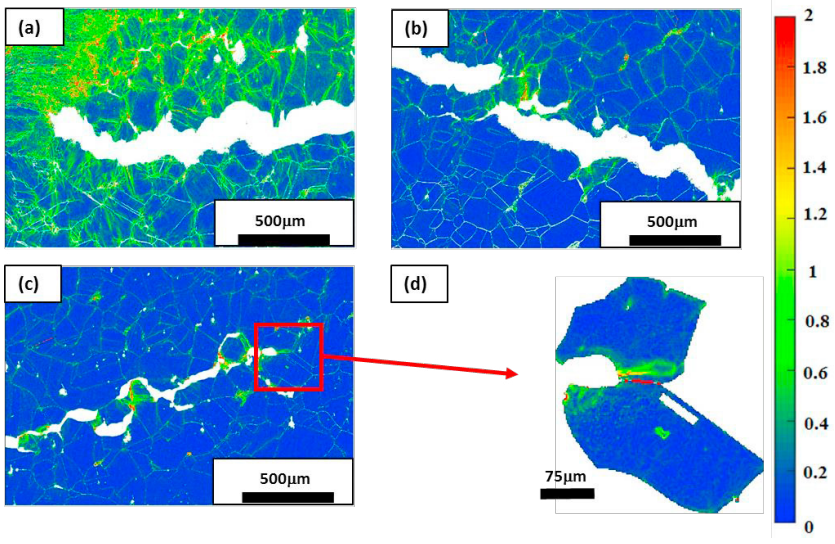

Figure 5. Kernel average misorientation (KAM) maps of the reheat crack at (a) location 1, (b) location 2, (c) location 3 and (d) magnified map of grains at the crack tip.

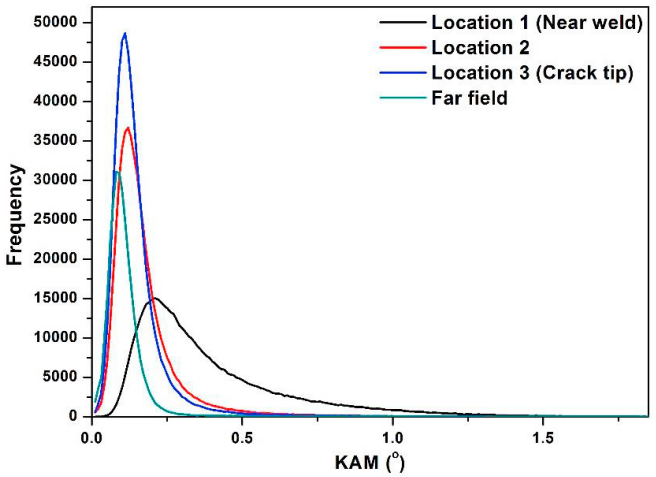

Figure 6. Frequency distribution of Kernel Average Misorientation (KAM) values at different locations.

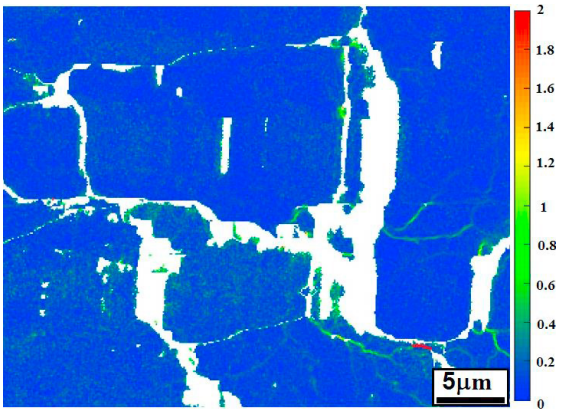

Figure 7. Kernel average misorientation (KAM) maps at cavities at higher magnification

The local deformation around the crack was also characterized by measuring Vickers hardness (HV). The micro-hardness contour maps (see Fig. 8) also showed higher hardnesses near the weld where the crack initiated. The misorientation and hardness maps are qualitatively similar to each other. Like some EBSD metrics, hardness values have been shown to be proportional to the square root of the dislocation density (Fujiyama et al., 2009b) but a direct correspondence between the two methods is limited by the difference in their spatial resolutions and the different extent of the strain fields they sample.

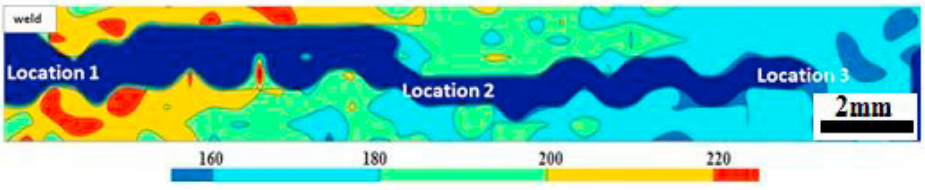

Figure 8. Hardness map around the reheat crack

GROD maps are helpful in visualizing the lateral spread of grains with high levels of intragranular misorientation. (see Fig. 9). These results were also consistent with the hardness map. Shigeyama et al. (Shigeyama et al., 2014) proposed that, during creep, voids form when $GROD_{ave}$ reaches a maximum value. So the lower GROD values towards the crack tip (see Fig. 11) can be associated with the reduction in the density of cavities. Damage assessment by small angle neutrons scattering (SANS) on a similar reheat crack on the same component has indicated a reduction in the cavity density towards the crack tip (Jazaeri et al., 2015). This evidence suggests that KAM and GROD maps might be correlated with cavity density.

An appropriate colour coding in the misorientation maps could help to reveal the extent of plastic deformation within each grain (Jin et al., 2013). Misorientation maps may also be helpful in predicting the direction of crack propagation but this needs further investigation. EBSD and micro-hardness are simple graphic methods for studying reheat cracks which illustrate the local dislocation density, but it is difficult to quantify the degree of deformation present as a reference unstrained condition must be defined (Wilkinson et al., 2010). There is considerable variation in the values given by both methods due to such factors as the crystal orientation, the grain geometry, the step size used and any strain induced by metallographic preparation.

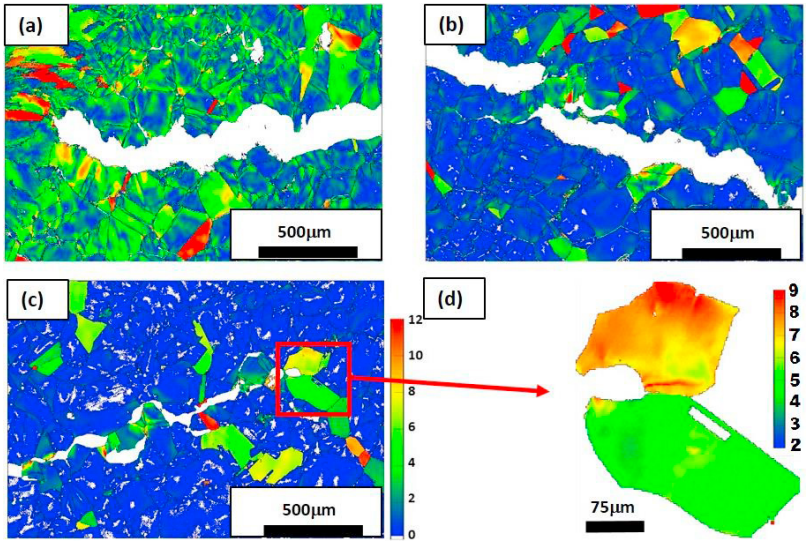

Figure 9. Intragranular misorientation (GROD) maps of the reheat crack at (a) location 1, (b) location 2, (c) location 3 and (d) magnified GROD map of grains at the crack tip on a different colour scale.

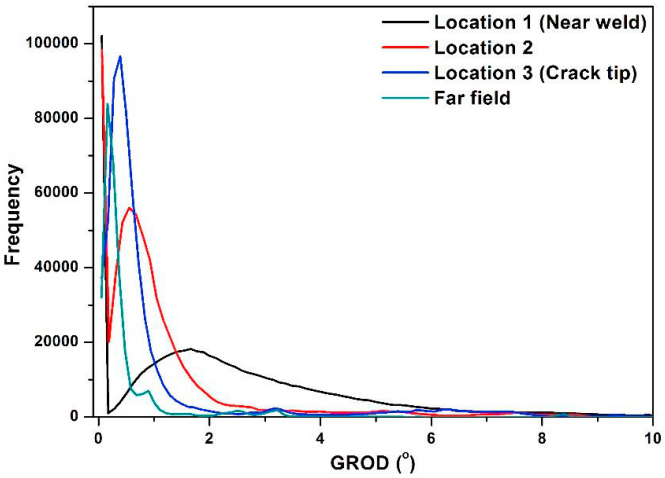

Figure 10. Frequency distribution of Grain Reference Orientation Deviation (GROD) values at different locations.

4. Conclusion

Plastic strain around a reheat crack in an ex-service type 316H austenitic stainless steel steam generator component has been studied using both EBSD and hardness mapping. The KAM and GROD maps revealed higher levels of lattice misorientation towards the weld region, where the crack initiated, with strain particularly concentrated at grain boundaries. The pattern of deformation shown by the EBSD measurements was confirmed by the hardness survey. Also KAM and GROD maps seem effective in identifying cavity nucleation sites in SEM images.

Acknowledgements

The authors would like to thank EDF Energy for funding the research and providing the sample studied.

References

Bouchard, P.J., Withers, P.J., McDonald, S.A., Heenan, R.K., 2004. Quantification of creep cavitation damage around a crack in a stainless steel pressure vessel. Acta Mater. 52, 23–34.

Brewer, L.N., Othon, M.A., Young, L.M., Angeliu, T.M., 2006. Misorientation Mapping for Visualization of Plastic Deformation via Electron Back-Scattered Diffraction. Microsc. Microanal. 12, 85–91.

Engler, O., Randle, V., 2010. Introduction to Texture Analysis, 2nd Editio. ed. Taylor & Francis Group, LLC.

Fujiyama, K., Harada, K., Ogawa, A., Kimachi, H., 2015. EBSD analysis of grain strain distribution for creep damaged SUS304HTB. J. Soc. Mater. Sci. Japan 64, 88–93.

Fujiyama, K., Mori, K., Kaneko, D., Kimachi, H., Saito, T., Ishii, R., Hino, T., 2009a. Creep damage assessment of 10Cr-1Mo-1W-VNbN steel forging through EBSD observation. Int. J. Press. Vessel. Pip. 86, 570–577.

Fujiyama, K., Mori, K., Matsunaga, T., Kimachi, H., Saito, T., Hino, T., Ishii, R., 2009b. Creep-damage assessment of high chromium heat resistant steels and weldments. Mater. Sci. Eng. A 510-511, 195–201.

Githinji, D.N., Northover, S.M., Bouchard, P.J., Rist, M.A., 2013. An EBSD Study of the Deformation of Service-Aged 316 Austenitic Steel. Metall. Mater. Trans. A 44A, 4150–4167.

Gottstein, G., Shvindlerman, L.S., 2010. Grain Boundary Migration Metals, 2nd Editio. ed. Taylor and Francis Group, LLC.

Jazaeri, H., Bouchard, P.J., Hutchings, M.T., Linder, P., 2014. Study of creep cavitation in a stainless steel weldment using small angle neutron scattering and Scanning electron microscopy, in: Proceedings of ASME 2014 Pressure Vessels & Piping Conference. ASME New York, p. V06AT06A037 1–6.

Jazaeri, H., Bouchard, P.J., Hutchings, M.T., Mamun, A.A., Heenan, R.K., 2015. Application of small angle neutron scattering to study creep cavitation in stainless steel weldments. Mater. Sci. Technol. 31, 535–539.

Jin, Y.J., Lu, H., Yu, C., Xu, J.J., 2013. Study on grain boundary character and strain distribution of intergranular cracking in the CGHAZ of T23 steel. Mater. Charact. 84, 216–224.

M'Saoubi, R., Ryde, L., 2005. Application of the EBSD technique for the characterisation of deformation zones in metal cutting. Mater. Sci. Eng. A 405, 339–349.

Schwartz, A.J., Kumar, M., Adams, B.L., Field, D.P., 2010. Electron Backscatter Diffraction in Materials Science, 2nd Editio. ed. Springer Science+Business Media, LLC.

Shigeyama, H., Sugiura, R., Matsuzaki, T., Yokobori, A.T., 2014. Micro- and macro-creep damage formation for P92 under multiaxial stress related to circular notched specimen. Mater. Sci. Technol. 30, 43–49.

Skelton, R.P., Goodall, I.W., Webster, G.A., Spindler, M.W., 2003. Factors affecting reheat cracking in the HAZ of austenitic steel weldments. Int. J. Press. Vessel. Pip. 80, 441–451.

Subedi, S., Pokharel, R., Rollett, A.D., 2015. Orientation Gradients in relation to grain boundaries at varying strain level and spatial resolution. Mater. Sci. Eng. A 638, 348–356.

Wilkinson, A.J., Clarke, E.E., Britton, T.B., Littlewood, P., Karamched, P.S., 2010. High-resolution electron backscatter diffraction: an emerging tool for studying local deformation. J. Strain Anal. Eng. Des. 45, 365–376.